Materials Research Express

RECEIVED
10 August 2017

REVISED
15 September 2017

ACCEPTED FOR PUBLICATION
19 September 2017

PUBLISHED
9 October 2017

PAPER

Crystal structure and high temperature Raman spectroscopy of Sr_2ZnTeO_6 double perovskite

Bouchaib Manoun[1,2], Y Tamraoui[1,2], I Saadoune[2,3], P Lazor[4] and W Yang[5] and J Alami[2,6]

[1] Univ Hassan 1er, Laboratoire des Sciences des Matériaux, des Milieux et de la modélisation (LS3M), 25000, Khouribga, Morocco
[2] Materials Science and Nanoengineering Department, University Mohamed VI Polytechnic, Lot 660—Hay Moulay Rachid, 43150 Benguerir, Morocco
[3] Laboratoire de Chimie des Matériaux et de l'Environnement (LCME), FST Marrakech, University Cadi Ayyad, Av. A. Khattabi, Marrakech 40000, Morocco
[4] Department of Earth Sciences, Uppsala University, SE-752 36, Uppsala, Sweden
[5] Center of High Pressure Science and Technology Advanced Research, Shanghai 201203, People's Republic of China
[6] Author to whom any correspondence should be addressed.

E-mail: jones.alami@um6p.ma

Keywords: double perovskite, phase transition, Raman spectroscopy, Sr_2ZnTeO_6

Abstract

Sr_2ZnTeO_6 double-perovskite oxide has been synthesized using solid state chemistry. As synthesized, the crystalline structure of Sr_2ZnTeO_6, refined using x-ray diffraction, is monoclinic having the space group $I2/m$. Structural phase transitions are studied using Raman spectroscopy in the temperature range 25 °C–567 °C. It is found that two of three observed bending Raman vibrations merge together at a temperature of around 120 °C, indicating a Sr_2ZnTeO_6 phase transition from the monoclinic ($I2/m$) to the tetragonal ($I4/m$). Furthermore, a temperature-dependence change-rate of external and O–Te–O bending modes and stretching modes are detected at 270 °C, which is interpreted as a phase transition from the tetragonal ($I4/m$) to the cubic (Fm-$3m$) structure.

1. Introduction

In the past decades, perovskites and double perovskites have been extensively investigated owing to their fascinating physical properties and potential applications. [1–9] It is well-known that the stability and the physical properties of double perovskites, $A_2BB'O_6$, are dependent on the nature of the constituent cations as well as on their structural characteristics. In particular, these types of compounds are influenced by the cation ordering, the octahedral distortion and the distribution of the B and B′ cations over the octahedral sites. Other parameters that control the properties of $A_2BB'O_6$ include the degree of cation inversion and the size and the electronic structure of the transition metal cations B and B′. Fundamental understanding of the structure stability and phase transitions of these materials, under different temperatures, is very important fundamental science and also for optimizing the next generation applications-tailored electronics.

First order phase transitions in perovskites can lead to the delimitation and deterioration of devices frequently heated or cooled through the transition. The question of the possible modifications of simple perovskite structures was first studied by Glazer [16]. He found 23 possible tilts of these octahedra. Then, by inspection, he assigned a space group to each of these possible tilts. Later, Woodward [17] generalized this classification scheme for the case of 1:1 ordered double perovskite materials ($A_2BB'X_6$). On the basis of group theory considerations, the number of possible space groups was reduced to 15 by Howard and Stokes [18], for the case of simple perovskite structures. Following the same formalism 12 possible space groups for the case of 1:1 ordering were identified [18].

In the last decades, excellent microwave properties have been reported for tellurium-based dielectric ceramics, sintered at relatively low temperatures (<700 °C) [8–11]. In most of those studied Te-based ceramics, Te exists in the 4 + valence state. However, stable Te-based double perovskite ceramics type A_2ZnTeO_6 (A = Ba, Sr,…) have Te in the 6 + valence state [12–15], which opens up for the possibility to develop materials with optimized microwave and electronic properties. The structure formation of the A_2ZnTeO_6 is yet to be understood, and conflicting results have been reported. For example, Ba_2ZnTeO_6 has been reported to have a hexagonal structure with space group $R3m$ [12], while Sr_2ZnTeO_6 has been found to be cubic [13] or as having a tetragonal symmetry (S.G. $I4/m$) [14, 15].

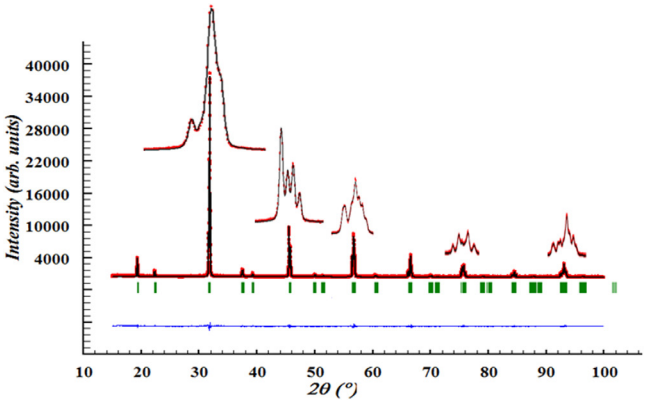

Figure 1. Final Rietveld plots for monoclinic Sr_2ZnTeO_6. The lower curve is the difference diagram showing a good agreement between the observed and calculated patterns.

Table 1. Details of rietveld refinement parameters for Sr_2ZnTeO_6-monoclinic phase.

Composition	Sr_2ZnTeO_6
Wavelength (Å)	$\lambda K\alpha 1 = 1.5406$
Step scan increment (°2θ)	0.010 142
2θ range (°)	15–100
Program	FULLPROF
Zero point (°2θ)	−0.0069 (7)
Pseudo-voigt function PV = $\eta L + (1-\eta) G$	$\eta = 0.5941(8)$
Caglioti parameters	$U = 0.0086$ (1)
	$V = -0.0031(1)$
	$W = 0.0046$ (3)
No. of reflections	152
No. of refined parameter	29
Space group	$I2/m$
a (Å)	5.6455(1)
b (Å)	5.6114(1)
c (Å)	7.9233(1)
β (°)	89.928(1)
V (Å^3)	251.003(5)
Z	2
Atom number	4
R_F	6.94
R_B	5.01
R_p	5.31
R_{wp}	7.39
cR_p	4.51
cR_{wp}	6.24

In the present work, high-quality single-phase Sr_2ZnTeO_6 is synthesized and the crystal structure is investigated, using x-ray diffraction (XRD). The structure stability, in the temperature range 25 °C–567 °C, is explored and two structural phase transitions are discovered at 120 °C and 270 °C, respectively. The discrepancies in claims by Dias *et al* [14], Dan *et al* [15], and Lentz [13] are clarified.

2. Methods

Sr_2ZnTeO_6 was prepared by conventional solid-state reaction from stoichiometric TeO_2 (99.9%) and ZnO (99.9%) with the appropriate metal carbonate $SrCO_3$ (99.9%). The samples were synthesized in air, in an alumina crucible, at a progressively high temperature sequence (600 °C/24 h, 800 °C/24 h, and 1000 °C/24 h) with intermediate regrinding. The chemical reaction is:

$$2SrCO_3 + ZnO + TeO_2 + 1/2O_2 \rightarrow Sr_2ZnTeO_6 + 2CO_2\uparrow.$$

Table 2. Refined structural parameters of the monoclinic Sr_2ZnTeO_6.

Atom	Site	*x*	*y*	*z*	*B* (Å)	Occupancy
Te	2*b*	0	½	0	0.40(4)	1
Zn	2*c*	½	0	0	0.65(7)	1
Sr	4*i*	0.5023(8)	½	0.2494(3)	0.71(4)	2
O1	4*i*	0.4556(2)	0	0.2603(2)	0.45(2)	2
O2	8*j*	0.2398(2)	0.2637(1)	−0.0316(1)	0.45(2)	4

Table 3. Selected inter-atomic distances (A°) and O–Te–O angles for Sr_2ZnTeO_6.

2 × Te–O1	1.916(9)
4 × Te–O2	1.911(8)
⟨Te–O⟩	1.9126
2 × Zn–O1	2.077(9)
4 × Zn–O2	2.100(8)
⟨Zn–O⟩	2.0923
2 × Sr–O1	2.819(1)
Sr–O1	2.589(8)
Sr–O1	3.059(7)
2 × Sr–O2	2.987(9)
2 × Sr–O2	2.617(9)
2 × Sr–O2	2.647(9)
2 × Sr–O2	3.008(9)
⟨Sr–O2⟩	2.817
1 × O1–Te–O1	180
2 × O2–Te–O2	180
4 × O1–Te–O2	87.9(7)
4 × O1–Te–O2	92.1(8)
2 × O2–Te–O2	92.1(6)
2 × O2–Te–O2	87.9(6)

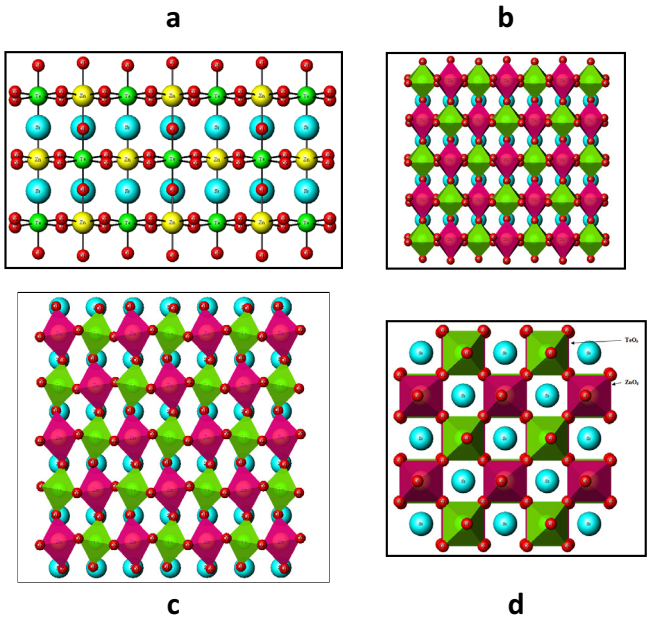

Figure 2. Projection of the unit cell illustrating the typical polyhedral arrangement and the tilt pattern (a). Also the (1 0 0) (b), (0 1 0) (c) and (0 0 1) (d) projections of the unit cell illustrate the typical polyhedral arrangement and the tilt pattern along the different axes.

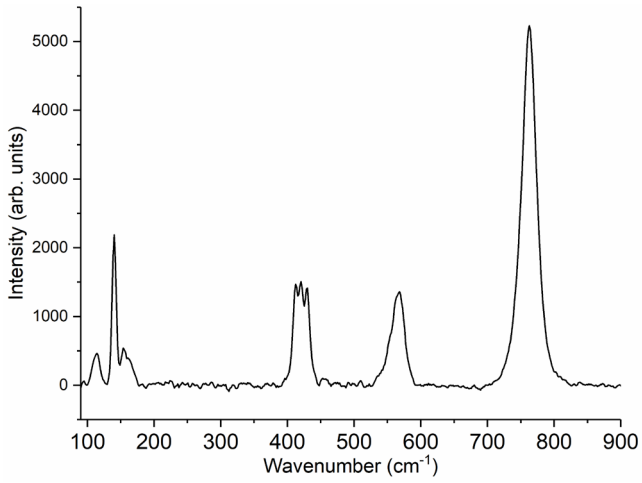

Figure 3. Raman spectrum of Sr_2ZnTeO_6 recorded at ambient conditions.

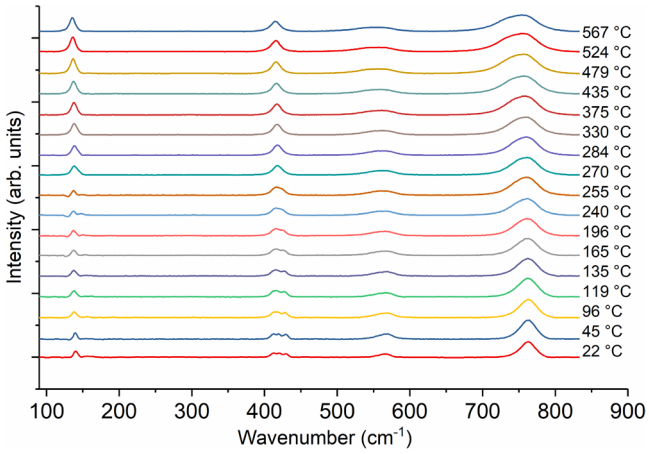

Figure 4. Raman spectra of Sr_2ZnTeO_6 versus temperature.

The structural refinement was undertaken from the powder x-ray data. A BRUKER-D2 Phaser (θ–θ) diffractometer in a Bragg–Brentano configuration was used to collect diffraction data at room temperature. Vibrational studies and high temperature phase transitions were performed using Raman spectroscopy. Details of the XRD and Raman spectroscopy experiment procedures are found elsewhere [19–21].

3. Results and discussion

X-ray powder diffraction patterns were indexed using Dicvol software [22]. The first 15 peak positions, with a maximal absolute error of 0.03° (2θ), were used as input data. It was found that the XRD patterns could be assigned to a monoclinic symmetry with the lattice parameters $a = 5.6455(1)$ Å, $b = 5.6114(1)$ Å, $c = 7.9233(9)$ Å, and $\beta = 89.928(1)°$, in agreement with previously reported results by Ubic *et al* [23] and Manoun *et al* [21]. In those studies, it was demonstrated that Sr_2MgTeO_6 favors an untilted to an in-phase-tilt transition (which lowers its symmetry to monoclinic ($I2/m$), rather than undergoing an antiphase to an in-phase tilt transition along the long axis.

The x-ray powder pattern of Sr_2ZnTeO_6 recorded at room temperature was refined with the Fullprof program [24], which is integrated in the Winplotr software [25] in order to minimize the profile discrepancy factor R_p. The refinement of the powder XRD pattern was carried out assuming a monoclinic lattice ($I2/m$) with the starting model taken from Manoun *et al* [21], where Sr^{2+}, Zn^{2+} and Te^{6+} occupy the 4*i* (x, 0.5, z), 2*a* (0.5, 0, 0) and 2*b* (0, 0.5, 0) sites, respectively; the oxygen atoms reside in 4*i* (x, 0, z) and 8*j* (x, y, z) positions. Figure 1 illustrates the observed, calculated, and difference patterns for Sr_2ZnTeO_6. A close inspection of the observed and calculated peaks reveal a good agreement between them (the insets show the zoomed-in details). Low residuals of the refinements could be deducted from the comparison presented in table 1, while the refined atomic positions in the monoclinic Sr_2ZnTeO_6 phase are listed in table 2. It is shown that Zn^{2+} and Te^{6+} cations are octahedrally

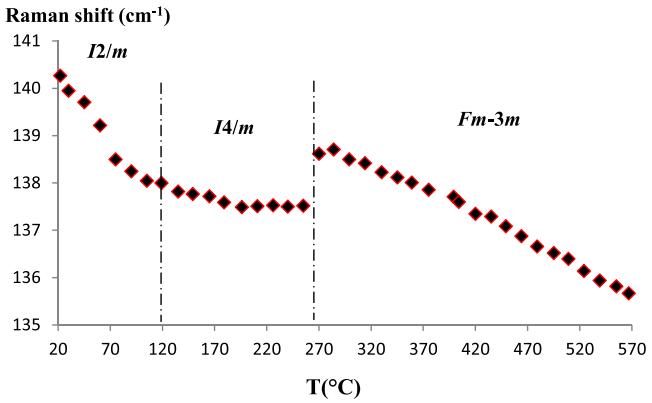

Figure 5. Raman lattice mode centered at 140 cm^{-1} of Sr_2ZnTeO_6 as a function of temperature. Clear slope changes are observed around 119 °C and 270 °C.

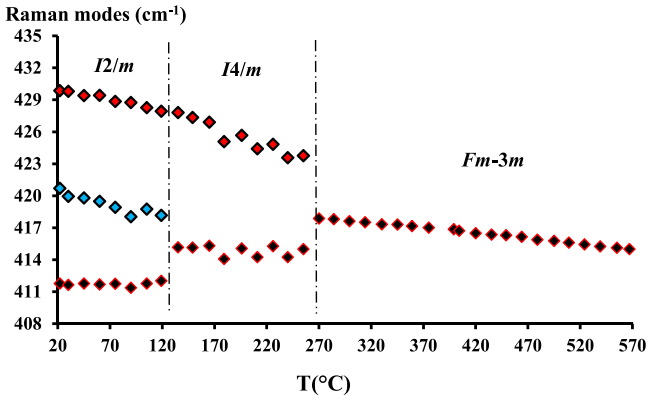

Figure 6. O–Te–O Raman bending modes of Sr_2ZnTeO_6 as a function of temperature. Discontinuity and slope change are observed indicating the occurrence of two phase transitions around 120 °C and 270 °C.

coordinated with the oxygen atoms, the ZnO_6 and TeO_6 octahedra alternatively connected and extended in three dimensions. Furthermore, Zn–O bond lengths are found to span the value-interval between 2.077 and 2.100 Å, while the Te–O bonds are almost equal in length, spanning the 1.911–1.916 Å range. Sr atoms were found to form SrO_{12} polyhedra with the Sr–O bond lengths in the 2.589–3.059 Å range. The inter-atomic distances are listed in table 3 and four projection views of the unit cell are shown in figure 2, where the typical polyhedral arrangement and the tilt pattern are clearly seen. Findings of this study are inconsistent with previous reports by Dias *et al* [14] and Dan *et al* [15] who claimed the tetragonal structure, and with Lentz [13], who solved the structure in a cubic system. Raman spectroscopy is used next to further illustrate these observations.

The room-temperature Raman spectrum of Sr_2ZnTeO_6 is shown in figure 3, where the Raman modes are of three types: lattice vibrations: (i) Sr^{2+} translations, and TeO_6 octahedra translational and rotational modes at wavenumbers below 200 cm^{-1}; (ii) O–Te–O bending vibrations, in the 200–500 cm^{-1} region, and (iii) Te–O stretching modes, at wavenumbers over 500 cm^{-1} [14, 26, 27].

The high sensitivity of Raman spectroscopy allows accurate determination of phase transitions by showing discontinuities in the composition, pressure or temperature dependences of the stretching, bending and external modes [28–31]. High temperature Raman spectra of Sr_2ZnTeO_6 were collected in the temperature range 25–567 °C, as shown in figure 4. The temperature-dependence of the external mode around 140 cm^{-1}, in the temperature range 25–567 °C, is presented in figure 5. Two changes in the slope are observed: the first at ~120 °C indicating the first phase transition from the monoclinic (*I*2/*m*) to the tetragonal (*I*4/*m*) structure, and the second, at ~270 °C. In figure 6, the bending modes centered at 420 cm^{-1} and 412 cm^{-1} are seen to merge to a combined mode centered at 415 cm^{-1}, at a temperature of ~120 °C, which is consistent with the *I*2/*m* to *I*4/*m* transition at the 140 cm^{-1} mode. At ~270 °C, the combined mode centered at 415 cm^{-1} merges with the 430 cm^{-1} mode giving rise to a new merged mode at ~418 cm^{-1} (figure 6), which indicates the occurrence of a second phase transition. This new mode wavenumber continuously decreases linearly upon temperature increase. Therefore, the temperature dependence of the intensity ratio of the modes 140 cm^{-1} and 762 cm^{-1}, I_{140}/I_{762}, is plotted as a reference. It is observed that this ratio is linearly proportional to the applied temperature, but exhibits a discontinuity in the slope at 120 °C and at 270 °C (figure 7); thus confirming the occurrence of both

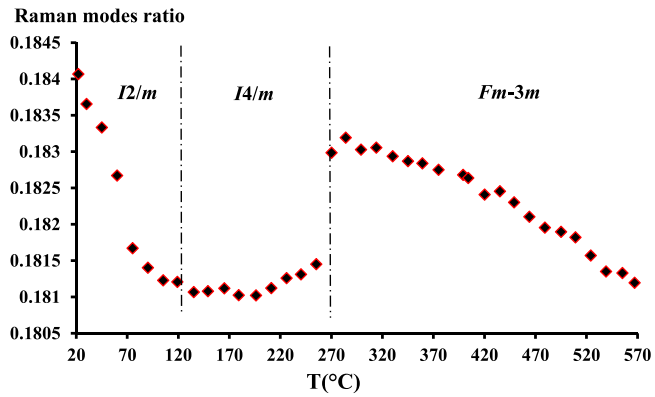

Figure 7. Raman modes ratio (140 cm^{-1}/762 cm^{-1}) as a function of temperature of Sr_2ZnTeO_6.

phase transitions. The transition from one system to the other is accompanied by a considerable change in the temperature dependence of this ratio around 120 and 270 °C (figure 7).

At room temperature, the Rietveld refinments shows that Sr_2ZnTeO_6 adopts a monoclinic system with the *I*2/*m* as a space group, which means that there is a combination of two out-of-phase tilts of equal magnitude around both a and b axes of the cubic cell. This happens with a tilt system $a^0b^-b^-$ according to Glazer notations [16], which is the equivalent of a single tilt, θ, around the [0 1 1] direction of the aristotype structure. The *I*2/*m* space group results from the combination of a rocksalt cation ordering and an $a^0b^-b^-$ tilting [16]. When increasing the temperature above 120 °C, the structure relaxes and only one single rotation of the octahedra around one of the fourfold axes is maintained, leading to a tetragonal symmetry with an out-of-phase rotation of the octahedra, $a^0a^0c^-$, and subsequently to a structure with *I*4/*m* symmetry. Futher increase of the temperature, above 270 °C, results in an undistorted aristotype Sr_2ZnTeO_6 rock-salt ordered perovskite structure with *Fm*-3*m* space-group symmetry; this untilted perovskite is assigned to the $a^0a^0a^0$ tilt system [16].

4. Conclusion

The systematic studies by XRD and Raman spectroscopy performed in the present work provide a detailed structural analysis of Sr_2ZnTeO_6, in the temperature range 25 °C–567 °C. It has been shown that phase changes occur as a function of temperature. At room temperature, the XRD and Raman data indicate the formation of a monoclinic Sr_2ZnTeO_6 with the space group *I*2/*m,* the same structure as Sr_2MgTeO_6 [21]. At 120 °C, the compound adopted a tetragonal structure. Upon further heating to above 270 °C, the cubic phase with the space group *Fm*-3*m* was observed. The high temperature phase transitions sequence for the studied compound is $I2/m \rightarrow I4/m \rightarrow Fm\bar{3}m$.

Acknowledgments

The authors are grateful to the University Hassan 1st for its support, the Office Chérifien des Phosphates in the Moroccan Kingdom (OCP group) and the Swedish Research Council for the financial grant SRL(MENA) # 348-2014-4287.

ORCID iDs

Y Tamraoui https://orcid.org/0000-0001-9121-2700
J Alami https://orcid.org/0000-0002-4919-5350

References

[1] Newnham R E and Ruschau G R 1991 *J. Am. Ceram. Soc.* **74** 463
[2] Cava R J, van Dover R B, Batlogg B and Rietman E A 1987 *Phys. Rev. Lett.* **58** 408
[3] Capponi J J *et al* 1987 *Europhys. Lett.* **3** 1301
[4] Gong G Q *et al* 1995 *Appl. Phys. Lett.* **67** 1783
[5] Ramesha K *et al* 2000 *Mater. Res. Bull.* **35** 559
[6] Nomura S, Toyama K and Kaneta K 1982 *Japan. J. Appl. Phys.* **21** 624
[7] Varma M R, Resmi R and Sebastian M T 2005 *Japan. J. Appl. Phys.* **44** 298
[8] Subodh G and Sebastian M T 2007 *J. Am. Ceram. Soc.* **90** 2266

[9] Udovic M, Valant M and Suvorov D 2001 *J. Eur. Ceram. Soc.* **21** 1735
[10] Kwon D K, Lanagan M T and Shrout T R 2005 *J. Am. Ceram. Soc.* **88** 3419
[11] Subodh G, Ratheesh R, Jacob M V and Sebastian M T 2008 *J. Mater. Res.* **23** 1551
[12] Von Rother H-J, Kemmler-Sack S and Fadin A 1977 *Z. Anorg. Allg. Chem.* **436** 213–6
[13] Lentz A 1972 *Z. Anorg, Allg. Chem.* **392** 218
[14] Dias A, Subodh G, Sebastian M T and Moreira R L 2010 *J. Raman Spectrosc.* **41** 702–6
[15] Dan-Dan H, Wei G, Na-Na L, Rui-Lian T, Hui L, Yan-Mei M, Qi-Liang C, Pin-Wen Z and Xin W 2013 *Chin. Phys.* B **22** 059101
[16] Glazer A M 1972 *Acta Cryst.* B **28** 3384–92
[17] Woodward P M 1997 *Acta Crystallogr.* B **53** 32
[18] Howard C J and Stokes H T 1998 *Acta Cryst.* B **54** 782–9
[19] Azdouz M, Manoun B, Azrour M, Bih L, El Ammari L, Benmokhtar S and Lazor P 2010 *J. Mol. Struct.* **963** 258
[20] Bih H, Bih L, Manoun B, Azdouz M, Benmokhtar S and Lazor P 2009 *J. Mol. Struct.* **936** 147
[21] Manoun B, Tamraoui Y, Lazor P and Yang W 2013 *Appl. Phys. Lett.* **103** 261908
[22] Boultif A and Louër D 1991 *J. Appl. Crystallogr.* **24** 987
[23] Ubic R, Letourneau S, Thomas S, Subodh G and Sebastian M T 2011 *J. Aust. Ceram. Soc.* **47** 49
[24] Rodriguez-Carvajal J 1990 *Collected Abstracts of Powder Diffraction Meeting (Toulouse, France)* vol 127
[25] Roisnel T and Rodriguez-Carvajal J 2001 *Mater. Sci. Forum* **378** 118
[26] Dias A, Subodh G, Sebastian M T, Lage M M and Moreira R L 2008 *Chem. Mater.* **20** 4347–55
[27] Haloui R *et al* 2017 *J. Appl. Surf. Interfaces* **1** 35–48
[28] Manoun B, Downs R T and Saxena S K 2006 *Am. Mineral.* **91** 1888–92
[29] Smit E, Manoun B and Waal D 2001 *J. Raman Spectrosc.* **32** 339–44
[30] Manoun B, Igartua J M, Gateshki M and Saxena S K 2004 *J. Phys.: Condens. Matter* **16** 8367
[31] Manoun B, Igartua J M, Gateshki M and Saxena S K 2008 *J. Mol. Struct.* **888** 244–52